Environ Earth Sci
DOI 10.1007/s12665-013-2888-8

ORIGINAL ARTICLE

Seawater inrush assessment based on hydrochemical analysis enhanced by hierarchy clustering in an undersea goldmine pit, China

Guoqing Li · Xinqing Wang · Zhaoping Meng · Haijun Zhao

Received: 26 April 2013 / Accepted: 25 October 2013

Abstract Seawater inrush is deadly to undersea mine and it is very important to accurately assess the connectivity between seawater and the mine pit. With Xinli gold mine area as a case study, following the analysis of geological setting, a detailed hydrogeological survey and sampling were conducted and conservative ions test of mine water samples was carried out in the laboratory. Furthermore, the physical significances of ion concentration and ion ratios, such as Cl^-, $\gamma SO_4^{2-}/\gamma Cl^-$ and $\gamma Na^+/\gamma Cl^-$, were checked. The test data analysis, enhanced by the physical significance check and hierarchy clustering analysis, was used to assess the overlying seawater inrush into the mine pit. It was determined that the undersea rock masses in the Xinli mine area bear high-mineralization brine water. The ore-controlling fault gouge and a thin layer of clay in Quaternary block the seepage of overlying seawater into the undersea mine pit to a great extent. The mine water from surrounding rock of the northeast gopher drift is closer to seawater in hydrogeochemical features, which indicates that the connectivity between the northeast of footwall of the ore-controlling fault and seawater is relatively good and should be closely monitored in future production. The mine water from the southwest gopher drift and crosscuts is similar to the brine (salty) water in chemical features, drains the net reserves of brine (salty) water in bedrock fissures and will impose few impacts on production in the near future. This approach is feasible and cost-effective.

Keywords Undersea mining · Hydrochemical features · Brine water · Connectivity · Desulphurization · Water–rock interaction

G. Li (✉) · X. Wang
Faculty of Earth Resources, China University of Geosciences, Wuhan 430074, Hubei, People's Republic of China
e-mail: ligq@cug.edu.cn

Z. Meng
College of Geosciences and Surveying Engineering, China University of Mining and Technology, Beijing 100083, People's Republic of China

H. Zhao
Key Laboratory of Engineering Geomechanics, Institute of Geology and Geophysics, Chinese Academy of Sciences, Beijing 100029, People's Republic of China

Introduction

Jiaodong Peninsula, located in east China, is rich in the precious metal, gold, with a proved reserve of up to 1,000 tons. A dozen goldmines are distributed over this coastal region where they are subjected to seawater intrusion or groundwater salinization. Groundwater salinization occurs in many coastal areas of the world. Due to various influencing factors, it is a big issue to determine the source and origin of salinization of a coastal aquifer. The hydrogeochemical processes affecting groundwater mineralization include: evaporation, dissolution of evaporate minerals, cation exchange with clay minerals, mixing processes related to seawater, deep brine water, return flow of agricultural irrigation, domestic and industrial waste waters (Salem et al. 2011; Mondal et al. 2011; Kim et al. 2012; Farid et al. 2013). Seawater intrusion is often linked to over pumping in coastal regions, leading to overdraft conditions and forming an inland gradient of seawater (Moujabber et al. 2006). Researchers proposed some criteria, such as Na/Cl, Ca/(HCO_3 + SO_4), to identify the origin of salinity, especially to determine the seawater intrusion in coastal aquifers. Although so far no severe water inrush has occurred in these mines, close attention must be paid to this issue.

Published online: 07 November 2013

The Xinli goldmine in northwest Jiaodong Peninsula, with its main ore body in the undersea rock masses, is the first gold mine exploited undersea in China (Fig. 1). It is also one of the largest goldmines in China with a proved reserve of over 30,000 kg of Au. Therefore, it is a big issue to assess the seawater inrush risk and to assure safe production.

Water inrush risk assessment is always a difficult problem, especially in coal mines. Previous studies indicated that a water inrush was usually controlled by three factors, including the water source, aquifuge and permeable channels. Researchers proposed several methods, such as a water inrush coefficient method, a vulnerable index method and so on, to assess the risk of water inrush in a coal mine (Aston and Whittaker 1985; Xu and Wang 1991; Zhang and Shen 2004; Yang et al. 2006; Meng et al. 2012). Geological conditions affecting water inrush in an undersea metal mine are quite different from that of a coal mine and few references can be obtained from approaches used in coal mine water inrush prevention. In addition, it is difficult to conduct routine geophysical surveys in the Xinli mine area as the ore deposits and tunnels are distributed in an undersea rock mass. Liu et al. (2007a, b) used stable isotope ^{18}O and water quality data to identify the mine water recharge sources of Sanshandao goldmine. Liu et al. (2012) studied the safety of undersea mining in the Xinli mine area using numerical simulation and suggested that it is safe to exploit the ore body below the −85 m level. Qian et al. (2008) utilized hydrochemical features, stable isotopes (δD and $\delta^{18}O$ values) and mine water temperature to analyze the hydrogeological conditions in Wang'ershan gold mine in Laizhou, China. Seki et al. (1986) and Mizukami et al. (1977) analyzed the submarine formation water at the Seikan undersea tunnel using geochemical methods. Isotopic and hydrochemical analysis was widely used in studies on seawater/saline intrusion and anthropogenic pollution of coastal aquifers (Duane et al. 1997; Zhang and Peng 1998; Guo 2004; Burnett et al. 2006; Ma et al. 2007; Yao et al. 2007; Güler et al. 2012; Povinec et al. 2012; Stoecker et al. 2013). With Xinli gold mine area as a case study, based on previous related research, the aim of the authors was to obtain a feasible approach to identify the seawater inrush passage in an undersea metal mine pit and thereby assess the seawater inrush risk.

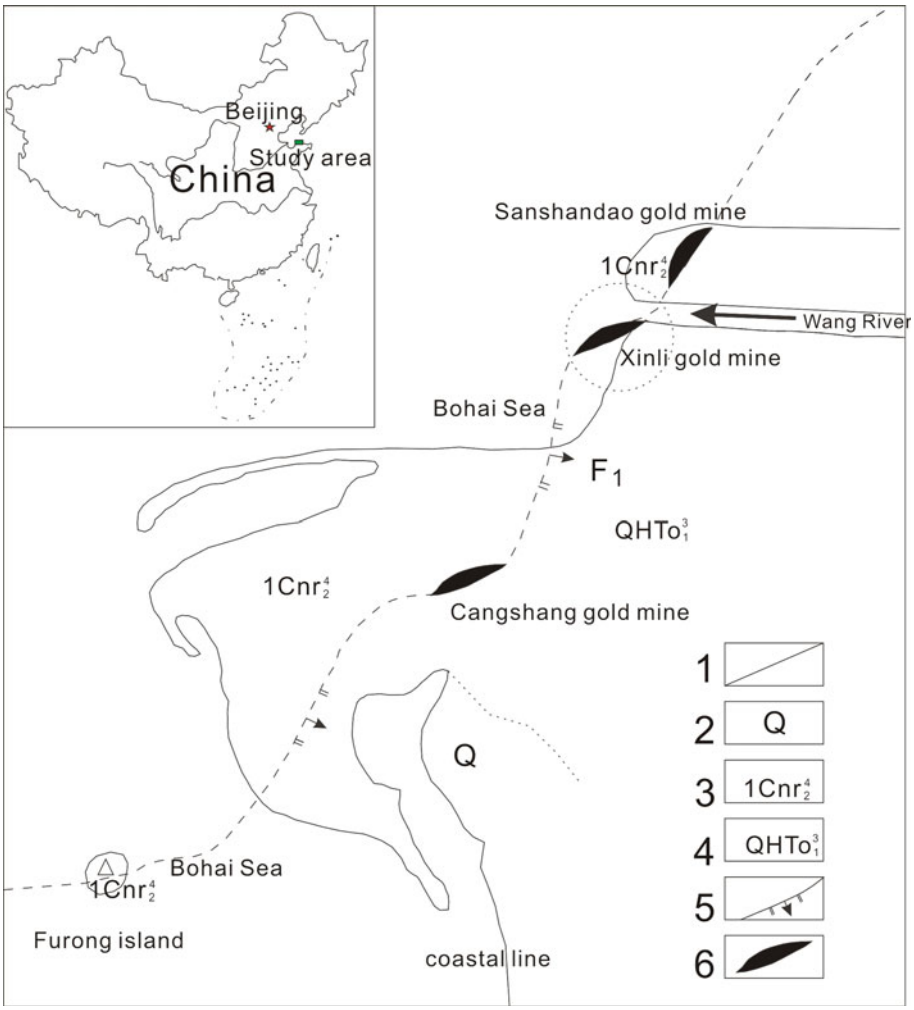

Fig. 1 Map showing location of the study area. *1* Coastline, *2* Quaternary, *3* Cuizhao unit of Linglong superunit, *4* Luanjiazhan unit of Malianzhuang superunit, *5* Fault, *6* Gold mine

Materials

Stratigraphic and geological structures

The Xinli mine area is situated near the Laizhou Bay, Bohai Sea. The elevation above sea level ranges from 1.2 to 4.5 m and overall tends to decreases from southeast to northwest. The Wang River runs across the northeast of Xinli mine area. The northwest of the mine area is covered by the Bohai Sea and both the ore deposits and ore-controlling structure F1 are undersea (Fig. 2). The overlying seawater is about 10 m deep. There are several fish ponds over the southeast of the mine area. The main, auxiliary, filling and ventilation shafts have been excavated and sublevel tunnels have been cut in −105, −135, −165, −200, −240, −280, −320, −360 and −400 m, and production test using the upward-filling mining method has been carried out in −200, −360 and −400 m sublevels (Fig. 3). The Sanshandao mine area is to the northeast of Xinli mine area (Zhao et al. 2011; Li et al. 2012).

Stratigraphically, the regional strata include the middle Archean Tangjiazhuang Group (Ar3t), new Archean Jiaodong Group (Ar4j), Paleoproterozoic Jingshan Group (Pt1j), Feizishan Group (Pt1f) and Quaternary System (Q) (Fig. 1). The unconsolidated sediment of Quaternary System is widely spread in the Xinli mine area and its thickness ranges from 8 to 10 m, with a maximum of 60 m. From bottom to up, the seabed Quaternary above the ore-bearing rock masses covers subclay, subsand, marine mud, silty clay, medium-fine sand, medium-coarse sand and coarse gravel (Sun et al. 2002).

Geotectonically, the Xinli mine area lies in the North Jiaodong uplift section of the North China platform. Old metamorphic basement of deformed rock masses, multi-stage and polygenetic magma activities and the NE-striking faults constitute the main Metallogenetic conditions. The Sanshandao–Cangshang fault F1 is the ore-controlling fault of the Sanshandao, Xinli and Cangshang gold mines (Fig. 1). The ore deposit in Xinli mine area belongs to structural hydrothermal alteration type. The mineralized alteration zone of the Xinli gold mine is 70–185 m wide and about 1,000 m deep (maximum). Lithologically, the alteration zone covers medium-fine grained metagabbro, Monzogranite granite, Cataclastic granite, Beresitization granite, and Beresitization cataclasite (Fig. 3). F1 stretches for 1,300 m in the direction of NE, dipping SE at an angle of 45°–75°. F1 strikes averagely N62°E in the west and N38°E in the east and extends for above 600 m in the deep. The Xinli fault F2, exposed by five wellbores, is located in the north of the Xinli mine area. It strikes N290°W and dips NE at an angle of 80°–90°.

Mechanically, F1 is a shear-compressional structure and F2 is an extensional one. Both F1 and F2 are of multi-stage tectonic activities. Generally, the joints are not well developed and the rock mass structure is a blocky type with RQD (Rock Quality Designation) values above 50 % and averaging around 85 %. The rock masses in Xinli mining area are hard ones. The uniaxial compressive strength of saturated medium-fine grained metagabbro, saturated sericitized granite and saturated Beresitization granite is around 51–86, 65–109 and 50–70 MPa, respectively. The geo-stress regime in Xinli mining area is dominated by

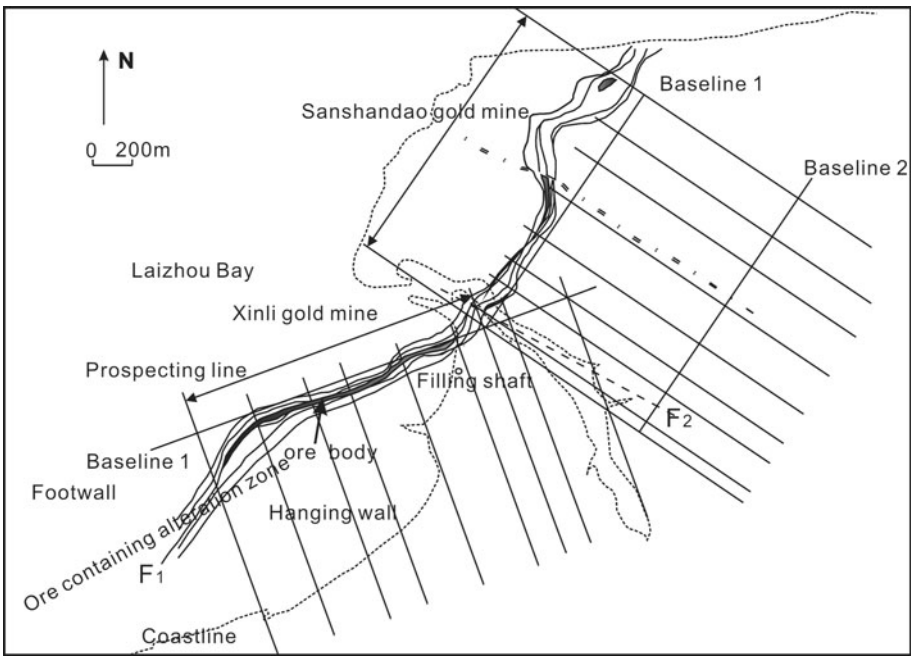

Fig. 2 Geological sketch of the Sanshandao-Xinli fault

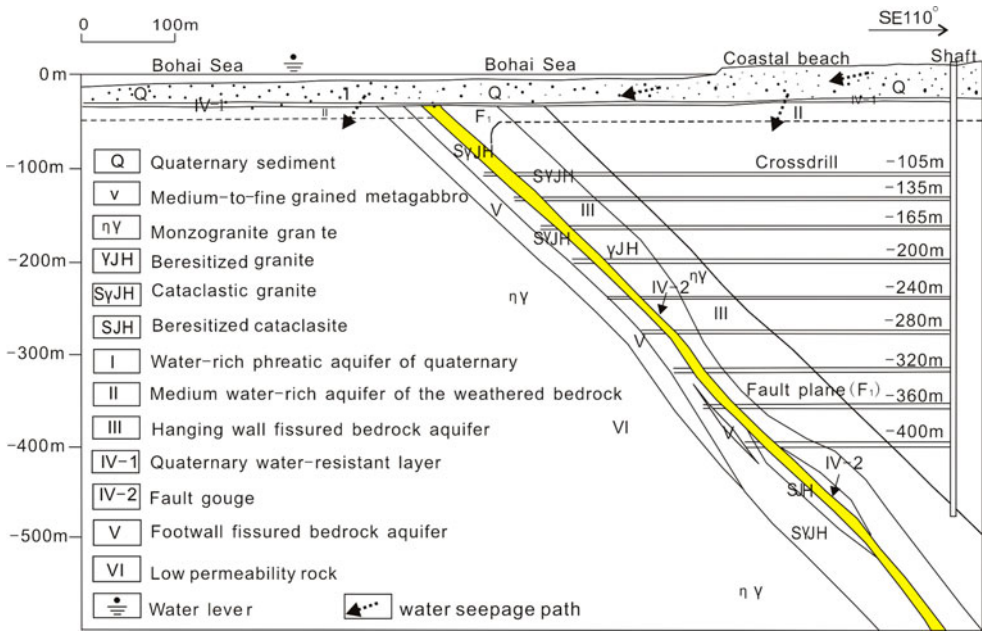

Fig. 3 Geological cross-section of the Xinli fault F1

horizontal tectonic stress, similar to that in Sanshandao mining area. The maximum and minimum principal stress is nearly horizontal and the maximum principal stress is in the direction of north by west, perpendicular to the ore-controlling fault F_1. Based on in situ measurements and regression analysis, Liu et al. (2012) described the geo-stress regime in Xinli mine area as follows:

$$\sigma_{h\max} = 0.11 + 0.0539H,$$

$$\sigma_{h\min} = 0.13 + 0.0181H,$$

$$\sigma_z = 0.08 + 0.0315H,$$

where $\sigma_{h\max}$, $\sigma_{h\min}$ and σ_z are the maximum horizontal principal stress, minimum horizontal principal stress, and vertical principal stress, respectively, Mpa; H is the buried depth of the measuring point, m.

Hydrogeological conditions

The hydrogeology is rather complex in Xinli mine area. The Wang River runs into the Bohai Sea during July and August annually and remains dry during the other months due to lack of precipitation. The runoff and discharge of pore water are poor due to the flat topography and the groundwater chemically features a Cl–Na type with the mineralization degree of 0.5–4.0 g/L. The Quaternary is rich in groundwater. Several sea fish ponds lie over the southeast of Xinli mine area. The possible water recharge sources of the Xinli mine pit include the surface Bohai Sea, Wang River, fish ponds over the mine area, groundwater in fractured rock masses and groundwater in Quaternary unconsolidated aquifer. The Bohai seawater is the greatest threat to the mine safety. The possible permeable channels are mainly rock fractures including F1, F2 and joints. On the whole, the rock mass is impermeable. But the relatively permeable part includes the Quaternary, the top weathered bedrocks, and fractured rock mass along the F1 and F2 fault planes. In situ hydraulic pressure test showed that the permeability coefficient of the weathered rock mass was 2.4e−7 m/s (Sun et al. 2002). There are fault gouges in both F1 and F2 fault planes. The F1 gouge is rich in clay minerals and about 0.05–0.1 m thick. The F2 gouge is dark gray mud and is about 0.02–0.1 m thick. The bottom layer of Quaternary, mainly composed of clay, silty clay and marine mud, is impermeable and blocks the contacts between the pore water, seawater and the fractured rock masses to some extent (Fig. 3). This layer is 0.8–10 m thick and the high variability of thickness casts doubts over the impermeability of this layer. Thereby, it is crucial to accurately predict the possible passage of seawater inrush.

Methods

Site fracture measurement and seepage survey

To identify the mine water recharge sources and to find out the connectivity between the mine pit and overlying modern seawater, a detailed hydrogeological survey and sampling work were carried out in cross drift, crosscut and gopher drift in −105, −135 m sublevels. A total of 1,135.1 m long roadway in −105 sublevel was surveyed and 19 water samples were collected from all the 196 seepage points; a total of 1,336.0 m long roadway in −135 sublevel was surveyed and 13 water samples were collected from all the 220 seepage points (Fig. 4). Seepage points in the roadway

Fig. 4 Sketch of hydrogeological survey in −105, −135 m level

are not distributed evenly and typical points were selected for sampling. Thirteen water samples were collected from surface Bohai Sea, Wang River, fish ponds over the mine area and drinking wells nearby, as well as of precipitation, respectively. Furthermore, a detailed joint investigation in the excavated roadways in all sublevels was carried out and over 5,000 joints were measured. The statistical results are shown in Fig. 5. Figure 5c, d shows that the prevailing orientation of joints in alteration zone (NW) is different from that in the surrounding rock of alteration (NE).

Water sampling in situ and conservative ions test in laboratory

All the 44 samples were tested hydrogeochemically in State Key Laboratory of Earthquake Dynamics (SKLED) Institute of Geology, China Earthquake Administration. Conservative ions in water samples were analyzed based on the standards of the People's Republic of China (GB7477-87, GB7476-87 and GB11899-89). The conservative ions Ca^{2+} and Mg^{2+} were analyzed using the EDTA titration method (GB7477-87, GB7476-87); K^{+} and Na^{+} were analyzed by flame atomic absorption spectrometry (GB11904-89); Cl^{-} was measured using the titration method; SO_4^{2-} was determined by the gravimetric method (GB 11899-89).

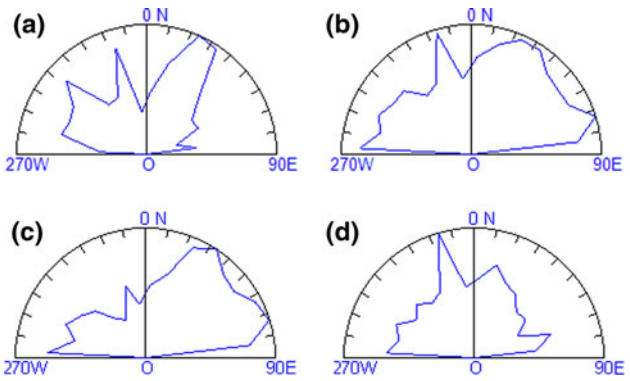

Fig. 5 Strike rose diagram of joints in, **a** hanging wall, **b** footwall, **c** surrounding rock of alteration zone in footwall and **d** alteration zone in footwall

Test data analysis enhanced by hierarchy clustering analysis

Usually, groundwater dynamics (water level and temperature) monitoring, and chemical analysis are used to identify the mine water sources of a pit. In case the inflow in a pit is small and temperature and chemical features of different possible sources do not differ significantly, some mathematical methods need to be used to determine an indicating index and thereby to assess the mine water sources.

Paleo-seawater infiltrated into the local fracture during marine ingression and experienced evaporation–concentration and salts may undergo hydrolytic dissociation processes during marine regression, and then turned into brine water gradually (Ma et al. 2007). In Xinli mine area, the net reserve and rate of brine seepage into mine workings are limited and do not threaten the production; however, the overlying seawater is dangerous. Due to the existence of the brine water, it is very hard to exactly determine the proportions of different water sources, especially seawater and, therefore, further analysis is necessary.

Table 1 Hydrogeochemical test data of water samples

Sample ID	Dissociated CO_2 (mg/L)	Mineralization degree(M) (g/L)	Cl^- {mg/L)	$SO4^{2-}$ (mg/L)	HCO_3^- (mg/L)	NO_3 (mg/L)	CO_3^{2-} (mg/L)	Na^+ (mg/L)	K^+ (mg/L)	Ca^{2+} (mg/L)	Mg^{2+} (mg/L)	Celsius temperature (°C)	Water chemical facies
W105-01	4.9	37.2	20,585.5	2,713.7	268.4	0	0	11,500	207.5	716.4	1,175.5	17	Cl–Na
W105-02	3.7	41.7	23,158.4	3,097.9	295.3	0	0	12,812.5	212.5	651.3	1,427.6	17.8	Cl–Na
W105-03	3.7	41.0	22,644	3,001.9	244	0	0	12,812.5	212.5	676.4	1,412.4	19	Cl–Na
W105-04	6.1	43.8	24,702.3	2,977.9	237.9	0	0	13,250	192.5	876.8	1,576.5	18.6	Cl–Na
W105-05	1.2	38.6	21,408.6	2,929.8	262.3	0	0	11,750	207.5	651.3	1,366.9	17.1	Cl–Na
W105-06	1.2	43.5	23,981.9	3,122	274.5	0	0	13,562.5	220	751.5	1,549.1	17.1	Cl–Na
W105-07	7.4	68.7	39,112.3	4,418.8	244	0	0	19,500	192.5	2,204.4	3,049.7	17	Cl–Na
W105-08	1.2	38.1	21,099.8	2,881.8	268.4	0	0	11,750	207.5	576.2	1,351.7	17	Cl–Na
W105-09	3.7	39.1	21,614.6	2,833.8	274.5	0	0	12,187.5	207.5	626.3	1,369.9	16.2	Cl–Na
W105-10	3.7	44.1	24,393.5	3,314.1	286.7	0	0	13,562.5	220	776.6	1,582.5	16	Cl–Na
W105-11	2.4	50.4	27,790.3	3,362.1	268.4	0	0	16,125	237.5	891.8	1,767.8	16	Cl–Na
W105-12	4.9	59.1	32,936.6	4,130.6	317.3	0	0	18,250	255	1,052.1	2,126.3	16	Cl–Na
W105-13	6.1	64.0	36,024.3	4,514.8	323.4	0	0	19,187.5	260	1,262.5	2,423.9	16	Cl–Na
W105-14	6.1	68.0	38,082.9	4,682.9	329.5	0	0	21,000	295	1,067.1	2,530.2	16	Cl–Na
W105-15	6.1	60.8	33,965.7	4,156	335.6	0	0	19,125	240	926.9	2,098.9	16.4	Cl–Na
W105-16	4.9	82.6	46,317.2	5,283.3	268.4	0	0	25,312.5	261	1,703.4	3,462.8	16	Cl–Na
W105-17	4.9	52.2	29,848.9	3,001.9	280.6	0	0	15,625	135	1,392.8	1,889.3	21.3	Cl–Na
W105-18	6.1	70.6	39,626.7	4,755	207.4	0	0	21,000	170	1,853.7	3,007.1	21.7	Cl–Na
W105-19	6.1	56.5	31,392.7	3,962.5	280.6	0	0	17,125	365	1,112.2	2,272.1	20.4	Cl–Na
W135-02	12.3	57.8	33,348.2	3,266	219.6	0	0	16,450	132	2,148.3	2,196.7	24.3	Cl–Na
W135-03	8.6	58.1	33,183.7	3,746.3	286.7	0	0	17,150	212	1,242.5	2,308.5	21.3	Cl–Na
W135-04	3.7	51.5	28,654.9	3,688.7	250.1	0	0	15,700.2	228	1,042.1	1,905.1	23	Cl–Na
W135-05	3.7	45.8	26,184.4	3,073.9	195.2	0	0	13,350	168	1,162.3	1,715.6	23	Cl–Na
W135-06	3.7	41.7	23,467.2	2,881.8	250.1	0	0	12,700	212	681.4	1,458.0	20.5	Cl–Na
W135-07	3.7	41.6	23,467.2	2,881.8	244	0	0	12,500	192	825.6	1,492.0	19	Cl–Na
W135-08	6.1	42.5	23,879.1	3,035.5	250.1	0	0	12,700	192	881.8	1,569.8	17	Cl–Na
W135-09	9.8	76.8	43,641.1	4,956.7	250.1	0	0	22,950	276	1,603.2	3,134.7	18.5	Cl–Na
W135-10	9.8	62.9	35,406.8	4,169	225.7	0	0	19,000	250	1,362.7	2,478.6	20.2	Cl–Na
W135-11	7.4	61.0	34,171.7	4,265.1	268.4	0	0	18,650	260	1,162.3	2,269.6	20.2	Cl–Na
W135-12	7.4	66.2	37,053.8	4,514.8	323.4	0	0	20,250	280.8	1,202.4	2,527.2	20	Cl–Na
W135-13	4.9	69.7	39,112.3	4,923.1	274.5	0	0	21,000	270	1,468.9	2,694.3	18.9	Cl–Na
Seawater1	3.7	30.0	16,468.3	2,439.9	158.6	0	0	9,050	362.5	380.8	1,125.1	22.8	Cl–Na
Seawater2	3.7	29.4	16,303.5	2,267.1	152.5	0	0	8,800	350	392.8	1,122.7	23.1	Cl–Na
Saline water1	13.5	38.4	20,585.5	2,881.8	317.3	0	0	12,625	222.5	551.1	1,184.6	17.6	Cl–Na

Table 1 continued

Sample ID	Dissociated CO_2 (mg/L)	Mineralization degree(M) (g/L)	Cl^- {mg/L)	$SO4^{2-}$ (mg/L)	HCO_3^- (mg/L)	NO_3 (mg/L)	CO_3^{2-} (mg/L)	Na^+ (mg/L)	K^+ (mg/L)	Ca^{2+} (mg/L)	Mg^{2+} (mg/L)	Celsius temperature (°C)	Water chemical facies
Saline water2	9.8	35.3	19,762	2,473.5	225.7	0	0	10,875	223.8	551.1	1,233.2	17.7	Cl–Na
Saline water3	6.1	28.1	15,233.2	2,401.5	183	0	0	8,437.5	354.4	450.9	1,063.1	19.5	Cl–Na
Saline water4	9.8	30.7	16,879.9	2,209.4	207.4	0	0	9,680	237.5	400.8	1,083.8	15	Cl–Na
Saline water5	11.5	31.4	17,456.3	2,228.6	176.9	0	0	9,750	362.5	320.6	1,093.5	18.1	Cl–Na
Freshwater1	4.9	0.6	89	76.8	140.3	0	0	59.8	1.4	100.2	14.6	17.8	Cl–HCO3–Ca–Na
Freshwater2	4.9	1.3	212.3	405.4	256.2	0	0	188.2	11.8	138.3	42.5	17.5	SO4–Cl–Na–Ca
Freshwater2	3.7	2.2	816.8	331.4	213.5	0	0	488	9.9	208.4	37.7	17.5	Cl–Na–Ca
Freshwater3	4.9	0.4	21.3	55.7	209.9	0	0	31.2	1	81.0	4.4	16.9	HCO3–Ca
Freshwater4	8.6	1.0	257	134.5	219.6	0	0	129.5	4.2	144.3	26.7	21.4	Cl–HCO3–Ca–Na
Surfacewater	6.1	0.1	10.6	9.6	46.4	0	0	15	2.7	6.2	2.3	20	HCO3–Na–Ca

Based on test data and previous studies (Duane et al. 1997; Wu et al. 1996; Liu et al. 2008; Belkhiri et al. 2012; Kim et al. 2012), the physical meanings of some variables are checked as follows:

(1) Cl^-

It is the most stable major element in seawater and cannot be adsorbed by plants, bacteria and soil. It is not easy to precipitate due to high solubility. The mineralization and electrical conductivity (EC) will rise with the increase of Cl^- concentration.

(2) $\gamma SO_4^{2-}/\gamma Cl^-$ (environmental index)

For waters, originated from the same source, the values of $\gamma SO_4^{2-}/\gamma Cl^-$, depending on reduction–oxidation environment, may be quite different. Specifically, Cl^- and SO_4^{2-} concentration cannot increase synchronically and even may change in reverse directions when water environment evolves from oxidation to reduction. The main reason for it is that water in a long-term sealed reduction environment will suffer desulfurization and SO_4^{2-} will be reduced to H_2S and S and lower the concentration thereof. Paleo-seawater may be concentrated due to evaporation and suffer desulfurization due to long-term sealed reduction environment and thereby the value of $\gamma SO_4^{2-}/\gamma Cl^-$ may differ from that of modern seawater in an open oxidation system.

Millimoles equivalent per liter (γ) equals milligram per liter multiplied by its atomicity and divided by its molecular weight. For instance, the concentration of SO_4^{2-} is 1,767.5 mg/L and its corresponding concentration in milligram equivalent per liter, γSO_4^{2-}, can be obtained by 1,767.5 (mg/L) $\times$ 2/98 = 36.071 meq/L.

(3) $\gamma Na^+/\gamma Cl^-$ (environmental index)

$\gamma Na^+/\gamma Cl^-$ of modern seawater equals to 0.85. Marine mud is rich in organic materials and various micro-organisms, and anoxic reducing environment thereof is conducive to biochemical reaction. Marine sedimentary water will be concentrated in lagoon and suffer desulfurization. The SO_4^{2-} concentration will drop and even diminish, which results in the emergence of H_2S, the increase of HCO_3^- concentration and the rise of pH value. Part of Ca^{2+}, Mg^{2+} will react with HCO_3^- and produce $CaCO_3$ and $MgCO_3$ precipitation; thus, Ca^{2+} and Mg^{2+} concentration will then drop and the cationic adsorption equilibrium between the water and mud will be broken. Some Ca^{2+} adsorbed by mud will migrate into water and some Na^+ in water will be adsorbed by mud. The Na^+-rich paleo-seawater will replace some Ca^{2+} with Na^+; therefore, Ca^{2+} will increase in the water in bedrock fissures and Na^+ will drop; and $\gamma Na^+/\gamma Cl^-$ will be less than that of modern seawater.

Laizhou corresponds to north temperate East Asian continental monsoon climate, with four distinct seasons and sufficient sunshine. The annual precipitation is about

610 mm and it is a semi-humid area. Therefore, currently no significant evaporation occurs. During infiltration, the water environment may change from an open oxidation environment to a sealed reduction environment.

According to the geological setting, the mine pit is under the Bohai Sea. Due to the clay layer existing in Quaternary and possible brine water in magmatic rock fissures, possible hydrogeochemical processes include cation exchange with clay minerals, mixing related to seawater, and brine water. Therefore, some indicators can be used to classify the mine waters.

Hierarchical clustering analysis (HCA) is an effective approach to merge individual sample into homogeneous groups successively (Menció and Mas-Pla 2008; Kurchikov and Plavnik 2009; Belkhiri et al. 2012). According to HCA, initially all samples are considered as individual groups and then these samples are connected to form clusters based on their distances step by step. Always the closest two samples are merged into one group. Finally, all samples are combined into one group. The hierarchy is often expressed using a dendrogram.

The distance between two samples is obtained using a Euclidean distance square (SED), defined as follows:

$$d_{ij} = \sum_{k=1}^{p} \left(X_{ik} - X_{jk}\right)^2, \quad (1)$$

where p is the number of variables, k is the sequence number of variables, i, j are sequence numbers of samples, X_{ik} is the kth variable value of the ith sample.

The distance between two groups use Ward's Method (WD), that is, the sum of deviations squares of samples within one group should be smaller and that of groups should be larger. Initially, each sample is regarded as a group and then the closest two groups are merge into one, which will produce the smallest increment of sum of deviation squares. Finally, all samples are combined into one group.

One shortcoming of HCA is that it cannot express the correlations of each variable of all samples. The variable number used in HCA can be one or more; however, the selected variables should be physically clear, easy to determine and the values of a variable of different samples should be significantly different. That is, the selected variables should not be linearly correlated and their values should be quite different for the samples of different groups. For instance, Cl^-, mineralization and electrical conductivity (EC) of water samples often show good linear correlations between each other; so only one of the three variables was selected.

The variable values should be standardized due to its wide range of variation in different groups. The authors utilized Z-Score method to standardize the values of each variable.

$$Z = (x - \text{mean}(x))/\text{std}(x) \quad (2)$$

where x is the original value of a variable, Mean(x) is the mean of all the values of a variable, Std(x) is the standard variation of all the values of a variable.

Results and discussion

Conservative ion test results

The test results are as follows (Table 1).

The conservative ions test data show that the hydrochemical features of these samples are quite different. Primarily, the mineralization and water quality type of

Table 2 Correlation matrix of hydrochemical variables of water samples

Correlation coefficient	EC	Mineralization (M)	HCO_3^-	Cl^-	SO_4^{2-}	CO_2	$\gamma SO_4^{2-}/\gamma Cl^-$	K^+	Na^+	Ca^{2+}	Mg^{2+}	$\gamma Na^+/\gamma Cl^-$
EC	1.000											
Mineralization (M)	0.987	1.000										
HCO_3^-	0.561	0.581	1.000									
Cl^-	0.987	1.000	0.572	1.000								
SO_4^{2-}	0.981	0.989	0.608	0.986	1.000							
CO_2	0.148	0.136	−0.037	0.141	0.083	1.000						
$\gamma SO_4^{2-}/\gamma Cl^-$	−0.674	−0.626	−0.282	−0.623	−0.646	−0.074	1.000					
K^+	0.657	0.613	0.295	0.603	0.679	0.077	−0.643	1.000				
Na^+	0.985	0.998	0.602	0.996	0.991	0.127	−0.633	0.630	1.000			
Ca^{2+}	0.857	0.881	0.391	0.888	0.823	0.218	−0.465	0.301	0.854	1.000		
Mg^{2+}	0.965	0.989	0.510	0.990	0.971	0.150	−0.578	0.574	0.981	0.910	1.000	
$\gamma Na^+/\gamma Cl^-$	−0.601	−0.558	−0.437	−0.556	−0.579	−0.061	0.832	−0.544	−0.557	−0.464	−0.524	1.000

Wang River water, precipitation, seawater were quite different, as follows, respectively: 1.0 g/L, Cl–Ca·Na (Wang River water); 0.1 g/L, HCO_3–Na·Ca (precipitation); 29.4 ~ 30.0 g/L, Cl–Na (seawater); the mineralization of Quaternary groundwater and mine water ranges from 0.4 ~ 38.4 g/L to 37.2 ~ 82.6 g/L separately, higher than that of overlying Bohai seawater in most cases. Obviously, mine water contains brine water. The K^+ concentration in mine water samples was much higher than that in seawater, showing rock can adsorb K^+ from water. It also indicates that K^+ is rather active in ionic exchange adsorption (Seki et al. 1986).

Hierarchical clustering analysis results

To determine the effective variables, a correlation analysis was conducted and a correlation matrix of variables was used (Table 2). It turns out that Cl^- shows good correlation with M, SO_4^{2-}, EC, Na^+ and Mg^{2+}; so, these variables should be omitted. CO_2 and HCO_3^- were also omitted due to their very low concentrations and chemical instability. Then Cl^-, K^+, Ca^{2+}, $\gamma SO_4^{2-}/\gamma Cl^-$ and $\gamma Na^+/\gamma Cl^-$ were selected as HCA variables and HCA produced a dendrogram (Fig. 6).

HCA indicates that in Xinli mine area, pore waters in the Quaternary unconsolidated aquifer, 01, 08, 09, 05, 03, 02, 10, 06, 04 samples in −105 m sublevel and 06, 07, 08 samples in −135 m sublevel were hydrochemically close to seawater (Figs. 5, 6).

In −105 m sublevel, the samples close to seawater were from gopher drift in the northeast of the foot wall of F1. The W105-07 is located in No. 12 cross drift and was quite different from seawater in hydrochemical features and had a very high mineralization.

In −135 m sublevel, the samples close to seawater were from gopher drift between No. 6 and No. 9 crosscut in the northeast of the bottom wall of F1. W135-09, located in No. 14 cross drift, was from the seepage of hanging wall and was quite different from seawater in hydrochemical features.

Geomechanically, a compressive fault is impermeable and an extensional one is permeable. F1 is a shear-compressional one, but F2 is an extensional one. The results from this study also proved that seawater seepage channels are mainly distributed in the rock mass in the northeast of the foot wall of F1 and near F2. However, currently the excavation scale is small and inflow of mine water is rather low; and thereby the seawater inrush risk is low in the near future.

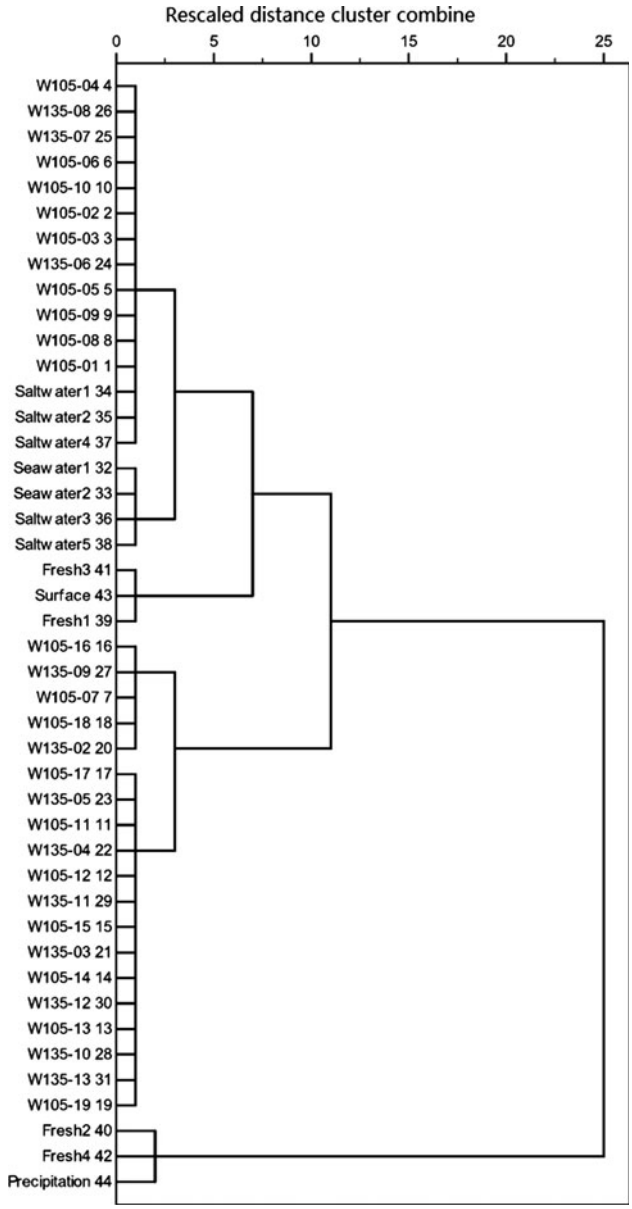

Fig. 6 Dendrogram of hierarchical clustering analysis result

Conclusions

The undersea rock masses in Xinli mine area bear high-mineralization brine water; the ore-controlling fault gouge and a thin layer of clay in Quaternary block the seepage of overlying seawater into undersea mine pit to a great extent.

The mine waters from surrounding rock of the northeast gopher drift and near the NW-trending fracture F2 are closer to seawater in hydrochemical features, which indicates that the connectivity between the northeast of foot-wall of the ore-controlling fault and seawater is relatively good and should be closely monitored in future production.

The mine waters from the whole hanging wall and the southwest of foot wall are mainly consuming the net reserve of brine in bedrock fissures, having little connectivity with overlying seawater and will impose few impacts on near future production.

The present seepage of overlying seawater into the mine pit was evaluated, and it can contribute to the issue of water disaster prevention in Xinli mine. The result is time-dependent. As the excavation goes on, the stress field and permeability of rock will change over time. Large-scale mining will change the stress field and generate new rock fissures or widen the existing fissures and thereby increase the risk level of seawater inrush. To ensure the production safety, regular hydrogeological monitoring and mine water quality tests should be continually conducted.

Cluster analysis is helpful for classification of mine water and for determining the seepage of seawater into the mine pit, but is not sufficient for the apportionment of the mine water sources. This approach is generally feasible and cost-effective.

Acknowledgments This study was financially supported by the Fundamental Research Foundation for National University, China University of Geosciences (Wuhan) under Grant No. CUGL120258, the National Basic Research Program of China (973 Program) under Grant No. 2012CB214705 and China Scholarship Council. The authors also thank the anonymous reviewers and editors for their efforts and help.

References

Aston TRC, Whittaker BN (1985) Undersea longwall mining subsidence with special reference to geological and water occurrence criteria in the North–East of England coalfield. Min Sci Technol 2(2):105–130

Belkhiri L, Mouni L, Boudoukha A (2012) Geochemical evolution of groundwater in an alluvial aquifer: case of El Eulma aquifer, East Algeria. J Afr Earth Sc 66–67:46–55

Burnett WC, Aggarwal PK, Aureli A (2006) Quantifying submarine groundwater discharge in the coastal zone via multiple methods. Sci Total Environ 367:498–543

Duane MJ, Pigozzi G, Harris C (1997) Geochemistry of some deep gold mine waters from the western portion of the Witwatersrand Basin, South Africa. J Afr Earth Sc 24(1):105–123

Farid I, Trabelsi R, Zouari K, Abid K, Ayachi M (2013) Hydrogeochemical processes affecting groundwater in an irrigated land in Central Tunisia. Environ Earth Sci 68:1215–1231. doi:10.1007/s12665-012-1788-7

Güler C, Kurt MA, Alpaslan M, Akbulut C (2012) Assessment of the impact of anthropogenic activities on the groundwater hydrology and chemistry in Tarsus coastal plain (Mersin, SE Turkey) using fuzzy clustering, multivariate statistics and GIS techniques. J Hydrol 414–415:435–451

Guo DF (2004) Principal component analysis on the ions in the groundwater intrusion area of Laizhou Bay. Marine Sci 28(9):6–9 (in Chinese)

Kim TH, Chung SY, Park N, Hamm SY, Lee SY, Kim BW (2012) Combined analyses of chemometrics and kriging for identifying groundwater contamination sources and origins at the Masan coastal area in Korea. Environ Earth Sci 67(5):1373–1388. doi:10.1007/s12665-012-1582-6

Kurchikov AR, Plavnik AG (2009) Clustering of groundwater chemistry data with implications for reservoir appraisal in West Siberia. Russ Geol Geophys 50:943–949

Li GQ, Ma FS, Meng ZP (2012) Analysis of connectivity between an undersea metal mine and overlying seawater in Xinli mine. J Central South University (Sci Technol) 43(10):3938–3945 (in Chinese)

Liu CP, Peng B, Qin JX (2007a) Geological analysis and numerical modeling of mine discharges for the Sanshandao Gold Mine: 1. Geological analysis. Mine Water Environ 26:160–165

Liu CP, Peng B, Qin JX (2007b) Geological analysis and numerical modeling of mine discharges for the Sanshandao Gold Mine: 2. Simulation and prediction of mine discharges. Mine Water Environ 26:166–171

Liu Q, Zheng XL, Ren JG et al (2008) Experimental study of column displacement in water-rock interaction during seawater intrusion. Marine Environ Sci 27(5):0443–0446 (in Chinese)

Liu ZX, Dang WG, He XG (2012) Undersea safety mining of the large gold deposit in Xinli District of Sanshandao gold mine. Int J Miner Metall Mater 19(7):574–583

Ma FS, Yang YS, Yuan RM et al (2007) Study of shallow groundwater quality evolution under saline intrusion with environmental isotopes and geochemistry. Environ Geol 51(6):1009–1017

Menció A, Mas-Pla J (2008) Assessment by multivariate analysis of groundwater–surface water interactions in urbanized Mediterranean streams. J Hydrol 352:355–366

Meng ZP, Li GQ, Xie XT (2012) A geological assessment method of floor water inrush risk and its application. Eng Geol 143–144:51–60

Mizukami M, Sakai H, Matsubaya O (1977) Na–Ca–Cl–SO_4-type submarine formation waters at the seikan undersea tunnel, Japan. Chemical and isotopic documentation and its interpretation. Geochimica et Cosmochimica Acta 41(9):1201–1212

Mondal NC, Singh VS, Saxena VK, Singh VP (2011) Assessment of seawater impact using major hydrochemical ions: a case study from Sadras, Tamilnadu, India. Environ Monit Assess 177:315–335. doi:10.1007/s10661-010-1636-8

Moujabber MEL, Bb Samra, Darwish T, Atallah T (2006) Comparison of different indicators for groundwater contamination by seawater intrusion on the lebanese coast. Water Resour Manag 20:161–180. doi:10.1007/s11269-006-7376-4

Povinec PP, Burnett WC, Beck A et al (2012) Isotopic, geophysical and biogeochemical investigation of submarine ground water discharge: IAEA-UNESCO intercomparison exercise at Mauritius Island. J Environ Radioact 10(4):24–45

Qian JP, Li SL, Cao C (2008) Geochemical characteristics and source analysis of inflow of mine water in Wang'ershan Gold Mine, Shandong. Chin J Geochem 27(1):82–89

Salem SBH, Moussa AB, Chkir N, Zouari K, Laure A, Cognard-Plancq AL, Marc V, Valles V (2011) Geochemical and isotopic investigation of groundwater mineralization process in the Zeroud basin, central Tunisia. Carbonates Evaporites 26:301–315. doi:10.1007/s13146-011-0058-1

Seki Y, Dickson FW, Liou JG et al (1986) Geochemical prediction of impending catastrophic inflow of seawater during construction of the undersea part of the Seikan Tunnel, Japan. Appl Geochem 1(3):317–333

Stoecker F, Babel MS, Gupta AD, Rivas AA, Evers M, Kazama F, Nakamura T (2013) Hydrogeochemical and isotopic characterization of groundwater salinization in the Bangkok aquifer system, Thailand. Environ Earth Sci 68:749–763. doi:10.1007/s12665-012-1776-y

Sun ZF, Zhu ZQ, Li W, et al. (2002) Geological exploration report of Xinli gold mine Laizhou Geological and Mineral Exploration Institute, Laizhou (in Chinese)

Wu JC, Xue YQ, Zhang ZH (1996) Experimental study on the cation exchange between water and rock in aquifer in the process of sea water intrusion. J Nanjing University (Nat Sci) 32(1):72–76 (in Chinese)

Xu XH, Wang J (1991) Prediction of coal mining water inrush. Geology publishing house (In Chinese), Beijing

Yang YG, Yuan JF, Chen SZ (2006) R/S analysis and its application in the forecast of mine inflows. J China Univ of Mining Tech (English Edition) 16(4):425–428

Yao J, Yu HJ, Wang SK et al (2007) The underground water hydrochemical characteristics of seawater invasion area around Laizhou Bay. Marine Sci 31(4):32–36 (in Chinese)

Zhang ZL, Peng LM (1998) The underground water hydrochemical characteristics on sea water intruded in eastern and southern coasts of Laizhou Bay. China Environ Sci 18(2):121–125 (in Chinese)

Zhang JC, Shen BH (2004) Coal mining under aquifers in China: a case study. Int J Rock Mech Min Sci 41:629–639

Zhao HJ, Ma FS, Li GQ et al (2011) Study of the hydrogeological characteristics and permeability of the Xinli Seabed Gold Mine in Laizhou Bay, Jiaodong Peninsula, China. Environ Earth Sci 65:2003–2014